AFGL-TR-84-0225
INSTRUMENTATION PAPERS, NO. 326

Fluxgate Magnetometer (SSM) for the Defense Meteorological Satellite Program (DMSP) Block 5D-2, Flight 7

FREDERICK J. RICH

25 July 1984

SPACE PHYSICS DIVISION PROJECT 2311
AIR FORCE GEOPHYSICS LABORATORY
HANSCOM AFB, MA 01731

This report has been reviewed by the ESD Public Affairs Office (PA) and is releasable to the National Technical Information Services (NTIS).

"This technical report has been reviewed and is approved for publication"

FOR THE COMMANDER

William J. Burke

WILLIAM J. BURKE, Branch Chf
Plasmas & Fields Branch
Space Physics Division

Rita C. Sagalyn

Rita C. Sagalyn, Director
Space Physics Division

Qualified requestors may obtain additional copies from the Defense Technical Information Center. All others should apply to the National Technical Information Service.

If your address has changed, or if you wish to be removed from the mailing list, or if the addressee is no longer employed by your organization, please notify AFGL/DAA, Hanscom AFB, MA 01731. This will assist us in maintaining a current mailing list.

Do not return copies of this report unless contractual obligations or notices on a specific document requires that it be returned.

Unclassified

SECURITY CLASSIFICATION OF THIS PAGE

REPORT DOCUMENTATION PAGE

1a. REPORT SECURITY CLASSIFICATION
Unclassified

1b. RESTRICTIVE MARKINGS

2a. SECURITY CLASSIFICATION AUTHORITY

2b. DECLASSIFICATION/DOWNGRADING SCHEDULE

3. DISTRIBUTION/AVAILABILITY OF REPORT
Approved for public release; distribution unlimited.

4. PERFORMING ORGANIZATION REPORT NUMBER(S)
AFGL-TR-84-0225
IP, No. 326

5. MONITORING ORGANIZATION REPORT NUMBER(S)

6a. NAME OF PERFORMING ORGANIZATION
Air Force Geophysics Laboratory

6b. OFFICE SYMBOL *(If applicable)*
PHG

7a. NAME OF MONITORING ORGANIZATION

6c. ADDRESS *(City, State and ZIP Code)*
Hanscom AFB
Massachusetts 01731

7b. ADDRESS *(City, State and ZIP Code)*

8a. NAME OF FUNDING/SPONSORING ORGANIZATION

8b. OFFICE SYMBOL *(If applicable)*

9. PROCUREMENT INSTRUMENT IDENTIFICATION NUMBER

8c. ADDRESS *(City, State and ZIP Code)*

10. SOURCE OF FUNDING NOS.

PROGRAM ELEMENT NO.	PROJECT NO.	TASK NO.	WORK UNIT NO.
61102F	2311	2311G2	2311G208

11. TITLE *(Include Security Classification)*
Fluxgate Magnetometer (SSM) (Contd)

12. PERSONAL AUTHOR(S)
Frederick J. Rich

13a. TYPE OF REPORT
Scientific. Interim.

13b. TIME COVERED
FROM ______ TO ______

14. DATE OF REPORT *(Yr., Mo., Day)*
1984 July 25

15. PAGE COUNT
28

16. SUPPLEMENTARY NOTATION

17. COSATI CODES

FIELD	GROUP	SUB. GR.
03	02	11
08	14	02

18. SUBJECT TERMS *(Continue on reverse if necessary and identify by block number)*
Ionosphere, Field-aligned currents, Aurora, Geomagnetic field, Space instrumentation, DMSP

19. ABSTRACT *(Continue on reverse if necessary and identify by block number)*

A triaxial fluxgate magnetometer has been successfully flown on a satellite of the Defense Meteorological Satellite Program. This instrument is sensitive enough to be used for scientific studies as well as for spacecraft operations. Unlike previous scientific-quality magnetometers in space, the sensor for this instrument is not mounted on a long boom but is mounted on the outer skin of the satellite, under the thermal blanket. While magnetic signals from the spacecraft are noticeable in the data, they do not significantly degrade the quality of the data. Algorithms are now available to process the magnetic field data in a "quick look" format. This enables a researcher to locate in the data the signature of disturbances in the earth's magnetic field due to geophysical events. In particular, the signature of field-aligned currents associated with high-latitude phenomena such as aurora can be found in the data.

Additional keywords: ionosphere; geomagnetic fields; F7 spacecraft.

20. DISTRIBUTION/AVAILABILITY OF ABSTRACT
UNCLASSIFIED/UNLIMITED ☒ SAME AS RPT. ☐ DTIC USERS ☐

21. ABSTRACT SECURITY CLASSIFICATION
Unclassified

22a. NAME OF RESPONSIBLE INDIVIDUAL
Frederick J. Rich

22b. TELEPHONE NUMBER *(Include Area Code)*
(617) 861-2431

22c. OFFICE SYMBOL
AFGL/PHG

DD FORM 1473, 83 APR — EDITION OF 1 JAN 73 IS OBSOLETE.

Unclassified

SECURITY CLASSIFICATION OF THIS PAGE

11. (Contd)

for the Defense Meteorological Satellite Program (DMSP) Block 5D-2, Flight 7

Contents

Illustrations

Illustrations

Tables

Fluxgate Magnetometer (SSM) for the Defense Meteorological Satellite Program (DMSP) Block 5D-2, Flight 7

1. INTRODUCTION

This is a status report on the triaxial fluxgate magnetometer flown on the Defense Meteorological Satellite Program (DMSP) Flight 7 (F7) in the Block 5D-2 series. The instrument is referred to as the SSM. The purpose of this report is to show the quality of data from the SSM and to provide information that users might need. The users will include scientists and programmers working with the F7 data, and engineering and technical personnel concerned with the operation of the F7 instrument and with a magnetometer on a future DMSP spacecraft.

The next section gives the purpose of the magnetometer on F7. Then a brief description of the DMSP satellite, the SSM instrument, and the SSM data processing are given. In the last section, some early orbit data are presented to show the quality and type of data that are expected from the SSM.

2. THE PURPOSE OF THE MAGNETOMETER ON A DMSP SPACECRAFT

Triaxial fluxgate magnetometers have been flown as scientific instruments on several previous spacecraft. These include the Air Force S3-2 spacecraft, the Navy TRIAD spacecraft, and the NASA MAGSAT and Dynamics Explorer spacecraft.

(Received for publication 12 July 1984)

All of these instruments showed that space-borne magnetometers could monitor geophysical disturbances related to disturbances in the ionosphere. All of these magnetometers were mounted on long booms to isolate them from spacecraft-induced disturbances. Body-mounted magnetometers on other spacecraft are used for attitude determination and other engineering functions. In some cases these body-mounted magnetometers have been used as scientific instruments, for example, on ISIS, S3-3 and Atmospheric Explorer. In all these cases, scientific data could only be recovered because the spacecraft was spinning, and recovery required a large amount of data analysis.

It is desirable to fly an operational magnetometer on DMSP spacecraft to monitor the geophysical environment, but engineering constraints prevent it from being mounted on a long boom. The SSM instrument was flown to prove that a scientific quality magnetometer could fly on an operational basis on DMSP spacecraft. Since there was some doubt whether or not useful data could be obtained from a body mounted sensor, the F7 instrument was flown on a proof-of-concept basis. The data shown herein illustrate that a body-mounted magnetometer can be used to investigate and monitor geomagnetic disturbances.

3. THE DMSP F7 SPACECRAFT

The F7 spacecraft was launched on 18 Nov 1983 into a 98.74 degree inclination, 456 nmi (844 km) by 444 nmi (822 km) orbit. The orbit is sun-synchronous with its ascending node at 1030 hours local time. On 22 Nov 1983, the SSM was turned on. Data are available starting 26 Nov 1983.

The DMSP Block 5D-2 spacecraft, including F7, are approximately 11.5 ft by 3 ft by 2 ft. Figure 1 shows a 5D-2 spacecraft in its flight configuration. The solar panel can pivot around two axes on the end of the boom to capture sunlight. The spacecraft coordinates are also shown in this figure. The +X axis is maintained in the down direction, the +Y is forward and +Z is maintained in the horizontal, cross-track direction. Attitude is maintained by four variable speed momentum wheels inside the spacecraft body. When the speed of any momentum wheel exceeds a desired level, current is applied to one of two wire coils creating a torque between the spacecraft and the earth's magnetic field. The roll/yaw torquing coil is in the X-Y plane of the spacecraft and the pitch torquing coil is in the X-Z plane of the spacecraft.

The primary mission of the DMSP spacecraft is to obtain tropospheric meteoro-ological data. The prime sensor for the DMSP mission is the Operational Line Scanner (OLS). This sensor images the earth below and to either side of the spacecraft in the visible-light and infra-red band. A photographic quality image of the

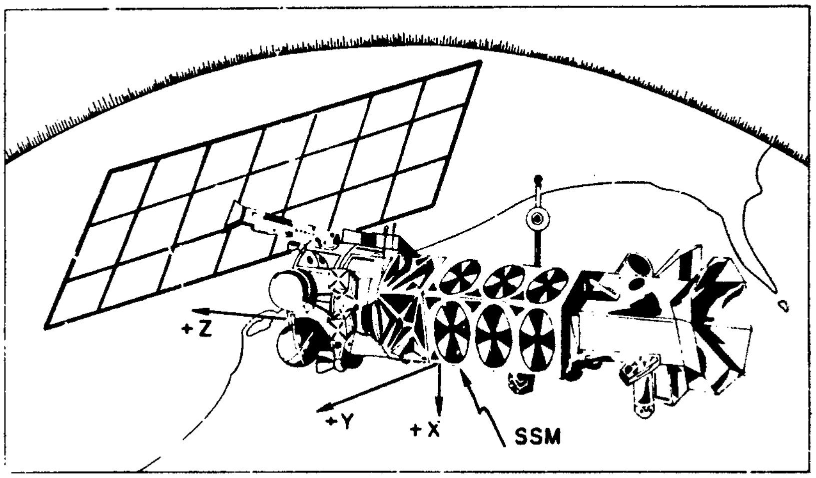

Figure 1. A DMSP Spacecraft From the Block 5D-2 Series, Which Includes the F7 Spacecraft That Carries the SSM. The spacecraft is shown in the flight configuration with the solar panel and the SSIE boom deployed. The SSM is on the +X surface of the spacecraft (not shown

earth below is built up by using the forward motion of the spacecraft to stack successive line scans. The principal purpose of the OLS images is to provide synoptic information about clouds. In the dark polar regions, the OLS images also provide information about the distribution and intensity of light from aurora. In addition to the OLS, DMSP spacecraft carry several other operational sensors that provide data about both the ionosphere-magnetosphere and the tropospheric environments. DMSP-F7 carries an SSJ/4 instrument, which measures precipitating 20 eV to 20 keV ions and electrons, and an SSIE instrument, which measures thermal ions and electrons. These instruments are of particular interest for on-going studies of ionosphere-magnetosphere processes. With these instruments and the SSM, it will be possibie to obtain a more complete specification of geophysical activity.

4. SSM INSTRUMENT CHARACTERISTICS

The SSM flown on DMSP F7 consists of two assemblies: a sensor assembly and an electronics assembly. The combined assemblies weigh less than 8 lb and draw less than 4 W. The sensor assembly consists of three separate single-axis fluxgate magnetometer units mounted in a brass fixture (Figure 2). The sensor units, built in the 1960's by Schonstedt Instrument Co., Reston, Virginia, were back-up units for Navy satellites developed by the Applied Physics Laboratory of Johns Hopkins University, Laurel, Maryland. The electronics unit was designed and built especially for the DMSP F7 spacecraft by the Applied Physics Lab. Mr. Kevin Heffernan was the project engineer.

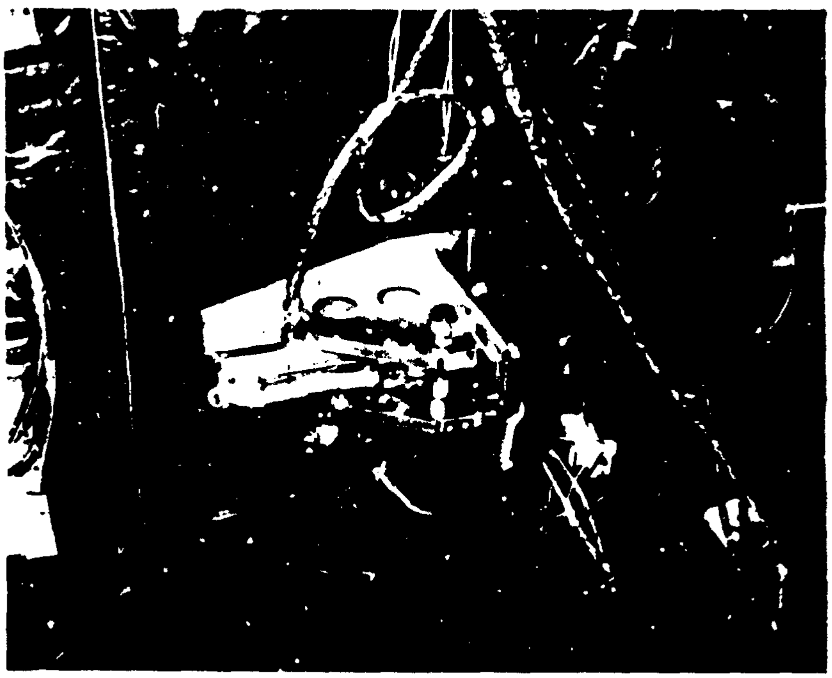

Figure 2. The Sensor Assembly of the Magnetometer (SSM) for DMSP F7. The assembly consists of three single-axis sensors mounted in a brass fixture so that the three sensors are mutually perpendicular. The SSM sensor assembly is shown mounted on the DMSP spacecraft with the thermal blanket laid back

The Applied Physics Lab has a long history of providing magnetometers for spacecraft. They have had technical responsibility for magnetometers on many Navy satellites starting in the 1960's. The magnetometer on the TRIAD satellite, the first instrument to conclusively determine the existence of field-aligned currents,[1]

1. Zmuda, A. J., and Armstrong, J. C. (1974) The diurnal variation of the region with vector magnetic field changes associated with field-aligned currents, J. Geophys. Res. 79(No. 16):2501-2502.

was the responsibility of JHU/APL. Design of the electronics was based on the design of the fluxgate magnetometer for MAGSAT, a NASA spacecraft flown in 1980 to survey the earth's magnetic field. This design was successfully used again by JHU/APL on the HILAT spacecraft launched in June 1983 for the Defense Nuclear Agency.

4.1 The Sensor Assembly

A fluxgate magnetometer sensor element consists of two wires wound around a mu-metal core. The first wire has an oscillating electrical current driven through it creating an electro-magnet which changes polarity direction at twice the drive frequency. The second wire winding is used to determine when the total magnetic field (the induced field plus the ambient field) is zero. With this measurement, the component of the ambient field parallel to the axis of the core is determined. To measure three components of the magnetic field vector, three sensor elements are needed. There are other techniques for sensing the ambient magnetic field, some of which measure the total field strength instead of the vector components. For a full description of magnetic field measuring systems used in space, see Ness.[2]

There is little difference between fluxgate magnetometers used for spacecraft operational functions and those used for scientific studies and/or environmental monitoring. The sensor elements are the same. The primary difference lies in the accuracy with which the field components are measured. For most operational requirements, a 1 percent accuracy is adequate and the measurements are made with a one-bit resolution of 500 nT. By comparison, the earth's magnetic field as measured on the ground is 35,000 nT near the equator and 70,000 nT near the magnetic poles. At the altitude of a DMSP satellite (830 km), the geomagnetic field strength is reduced by 35 percent.

The measurement accuracy of a scientific magnetometer must be much greater. The degree of accuracy is determined by the purpose of the measurement. For SSM, the primary scientific goal is to measure changes in the earth's magnetic field due to geomagnetic storms and substorms. These geophysical events are recorded by a satellite magnetometer as changes of a few nano Tesla to as much as 1000 nT during time intervals of a few seconds to a few minutes. To obtain sufficient accuracy in the data, the SSM was designed to measure changes in the geomagnetic field with a one-bit or one-count resolution of 12 nT per axis, at a rate of 20 samples/sec. The three axes of the sensor unit are mutually perpendicular within an accuracy of 0.1 deg. The attitude of the spacecraft is maintained in local vertical at all times with an accuracy better than 0.1 deg.

---

2. Ness, N.F. (1970) Magnetometers for space research, Space Sci. Rev., **11**:459-554.

Since the SSM was not intended to survey the main geomagnetic field, the instrument was not calibrated against standard field strengths with high accuracy on the ground and there is no provision for in-flight re-calibration. Thus, there may be an offset of approximately 200 nT per axis in the measurements from SSM The sensor unit may also be misaligned from the spacecraft coordinate system by as much as 0.1 deg per axis. This can cause an offset in the X and/or Y component of the measured field of as much as 0.2 percent of the main magnetic field or +100 nT to -100 nT. Also, bending of the spacecraft body may misalign the SSM from the spacecraft coordinate system by an additional 0.1 deg per axis.

4.2 The Electronics Assembly

The electronics of the SSM consists of two sections. An analog section detects the signals returned from the second winding of each sensor. These signals are converted into analog voltages proportional to the components of the ambient magnetic field. These analog measurement signals and analog signals, to show the instrument status, are sent directly to the Operational Line Scanner (OLS) subsystem which incorporates these with other engineering data. All of these signals are listed in Table 1. The second section converts the analog signals into digital signals to be incorporated into the digital telemetry.

Table 1. Analog Data From SSM

Word	Range	Transfer Function
X Magnitude	+/- 50,000 nT	4.6887×10^{-5} V/nT * Bx + 2.4682 V
Y Magnitude	+/- 50,000 nT	4.5998×10^{-5} V/nT * By + 2.4396 V
Z Magnitude	+/- 50,000 nT	4.6817×10^{-5} V/nT * Bz + 2.4730 V
Current Monitor	0 to 250 mA	1.9165×10^{-2} V/mA * I + 0.0213 V
5 Volt Supply	0 to 7.5 V	0.66667 V/V * V(5V)
Sensor Temperature	-25 to +50 C	4.3 V = -10 C; 1.0 V = 30 C
Electronics Temperature	-25 to + 50 C	1.3 V = -10 C; 4.5 V = 30 C

Since there is a requirement to provide a resolution of 12 nT per count, either the range of the analog signal had to be adjusted so that a standard 8-bit or 9-bit analog-to-digital (A-to-D) conversion would yield the required resolution or more bits per conversion had to be used. If the first option were chosen, the sensor would saturate at +/-3000 nT (+/-256 counts X 12 nT/count). This is reasonable when Helmholtz coils are wrapped around the sensor units to nullify the geomagnetic field, but not feasible due to weight and time requirements of the project. Thus the second option was chosen. The SSM analog signals are A-to-D converted using a 13-bit word. (Actually, the circuit uses a 16-bit A-to-D conversion with the 3 least significant bits (LSB) discarded.) The only difficulty in getting a 13-bit resolution is that the analog signals must be noise-free to better than one part in 8000. As shown below, this requirement was met.

Once the 13-bit digital data is obtained, it goes to a microprocessor for data compression. This makes it possible to get 780 bits/sec of data into a 360 bits/sec telemetry assignment. The compression scheme consists of outputting one 13-bit word each half second on each axis. The next 9 words per axis consist of 5-bit words that represent the difference between that sample's 13-bit value and the 13-bit value from the previous sample. That allows a change of 200 nT in each sampling period (1/20 sec). If the measured field changes faster than 200 nT in 1/20 sec, the 5-bit word is meaningless but a flag is set to warn the user of the problem. In practice, this only occurs when the torquing coils on the spacecraft are turned on or off, resulting in a loss of 2 or 3 seconds of data per orbit.

The format of the digital data after data compression is shown in Table 2. Negative values for the 13-bit and 5-bit words are given using two's-complement numbers. Unfortunately, Table 2 does not exactly represent the raw data. Due to a misunderstanding in how an experiment should interface with the OLS, each 36 bits of data are in reverse order and are complemented. Software in post-flight analysis easily takes care of properly reconstrucing the 13-bit words to represent the in-flight measurements

5. DATA ANALYSIS

The analog and digital data from the SSM are processed in two different ways. The analog data are separated from the digital data as soon as they are received by the Air Force Global Weather Central (AFGWC). Analog data go to the 1000th Satellite Operations Group (SOG) which has day-to-day responsibility for the DMSP spacecraft in flight.

Table 2. SSM Digital Data Format

Bits	Description
0-12	X Magnetometer set 1 base value 1
13-17	X Magnetometer set 1 delta 1 = value 1 - value 2
18-22	X Magnetometer set 1 delta 2 = value 2 - value 3
23-27	X Magnetometer set 1 delta 3 etc.
28-32	X Magnetometer set 1 delta 4
33-37	X Magnetometer set 1 delta 5
38-42	X Magnetometer set 1 delta 6
43-47	X Magnetometer set 1 delta 7
48-52	X Magnetometer set 1 delta 8
53-57	X Magnetometer set 1 delta 9
58-70	Y Magnetometer set 1 base value 1
71-75	Y Magnetometer set 1 delta 1
76-80	Y Magnetometer set 1 delta 2
81-85	Y Magnetometer set 1 delta 3
86-90	Y Magnetometer set 1 delta 4
91-95	Y Magnetometer set 1 delta 5
96-100	Y Magnetometer set 1 delta 6
101-105	Y Magnetometer set 1 delta 7
106-110	Y Magnetometer set 1 delta 8
111-115	Y Magnetometer set 1 delta 9
116-128	Z Magnetometer set 1 base value 1
129-133	Z Magnetometer set 1 delta 1
134-138	Z Magnetometer set 1 delta 2
139-143	Z Magnetometer set 1 delta 3
144-148	Z Magnetometer set 1 delta 4
149-153	Z Magnetometer set 1 delta 5
154-158	Z Magnetometer set 1 delta 6
159-163	Z Magnetometer set 1 delta 7
164-168	Z Magnetometer set 1 delta 8
169-173	Z Magnetometer set 1 delta 9
174-175	SPARE
176-188	X Magnetometer set 2 base value 1
189-193	X Magnetometer set 2 delta 1
194-198	X Magnetometer set 2 delta 2
199-203	X Magnetometer set 2 delta 3
204-208	X Magnetometer set 2 delta 4
209-213	X Magnetometer set 2 delta 5

Table 2. SSM Digital Data Format (Contd)

Bits	Description
214-218	X Magnetometer set 2 delta 6
219-223	X Magnetometer set 2 delta 7
224-228	X Magnetometer set 2 delta 8
229-233	X Magnetometer set 2 delta 9
234-246	Y Magnetometer set 2 base value 1
247-251	Y Magnetometer set 2 delta 1
252-256	Y Magnetometer set 2 delta 2
257-261	Y Magnetometer set 2 delta 3
262-266	Y Magnetometer set 2 delta 4
267-271	Y Magnetometer set 2 delta 5
272-276	Y Magnetometer set 2 delta 6
277-281	Y Magnetometer set 2 delta 7
282-286	Y Magnetometer set 2 delta 8
287-291	Y Magnetometer set 2 delta 9
292-304	Z Magnetometer set 2 base value 1
305-309	Z Magnetometer set 2 delta 1
310-314	Z Magnetometer set 2 delta 2
315-319	Z Magnetometer set 2 delta 3
320-324	Z Magnetometer set 2 delta 4
325-329	Z Magnetometer set 2 delta 5
330-334	Z Magnetometer set 2 delta 6
335-339	Z Magnetometer set 2 delta 7
340-344	Z Magnetometer set 2 delta 8
345-349	Z Magnetometer set 2 delta 9
350	TLM counter flag (nominally 0)
351	PROM flag (nominally 0)
352	Set 1 X overrange (nominally 0)
353	Set 1 Y overrange (nominally 0)
354	Set 1 Z overrange (nominally 0)
355	Set 2 X overrange (nominally 0)
356	Set 2 Y overrange (nominally 0)
357	Set 2 Z overrange (nominally 0)
358	Toggle flag (alternates between 0 and 1 each second)
359	Data useful flag (nominally 1)

5.1 Analog Data

Analog data are displayed on a ground controller's console in either numerical or graphical format. One such graph of the early SSM data is shown in Figure 3 together with tell-tales or indicators of activity of the two torquing coils used to maintain spacecraft attitude. Traces 1, 2 and 3 in Figure 3 represent the X, Y and Z magnetic field measurements. As an aid to the reader, the letters X, Y and Z have been written next to the appropriate magnetometer traces. Traces 4 and 5 are the tell-tales of the roll/yaw and pitch torquing coils respectively. Rises of either tell-tale from its base levels indicate that the roll/yaw or pitch coil was on. The height of the rise indicates the polarity of the current in the coil. For this period, the pitch coil was active five times and the roll/yaw coil was never on. While the pitch coil was active, there is a noticeable shift in the three outputs from the all three SSM sensors. It should be noticed that at no time in Figure 3 does the active coil cause any of the measurements of SSM to go off scale. This is true in the vast majority of cases when the coils are active.

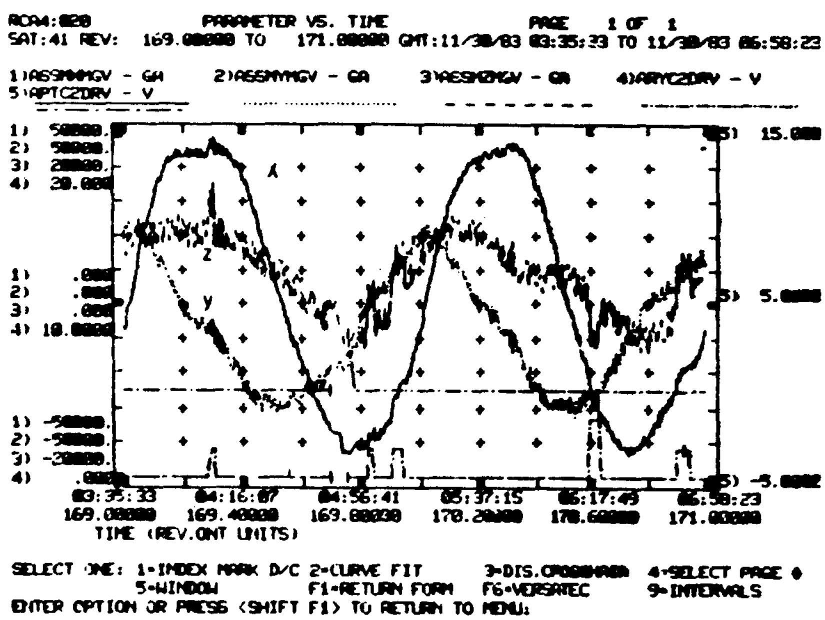

Figure 3. The SSM Magnetic Field Measurements (Traces 1, 2, and 3) and the Spacecraft Torquing Coil Tell-Tales (Traces 4 and 5) for Two Orbits on 30 Nov 1983. This figure is a copy of the analog telemetry values displayed on the consoles at the 1000th SOG

The analog outputs from the SSM seem to have a noise level of a few thousand nT. If this were true of the digital data, geophysical activity causing changes of a few hundred nT or less would be impossible to detect. In fact, this is not the case.

5.2 Digital Data

The digital data from a DMSP spacecraft are sent to the AFGWC's UNIVAC computer system along with all other digital data. Since the SSM is not an operational sensor, the F7 SSM data are not usually processed at AFGWC. The data are copied onto archive tapes each day and sent to the Air Force Geophysics Laboratory (AFGL) for processing. The first task of the AFGL staff was to determine if the quality of the SSM data was adequate for scientific studies. Dumps of the early, raw data showed an apparently random variation of about one count in the data. In fact, the variation has a periodicity of about one-half second. After taking arithmetic averages of each half second of data, the digital data as shown in Figure 4 has no noticeable instrumental variations. The level of the three signals have been shifted artificially so they can all be shown with a common scale. The 2 min of data in Figure 4 are part of the same data displayed in Figure 3. The trends in the measurements from the X, Y and Z sensors are due to changes in the location of the satellite. The variation in the Z sensor of approximately 10 counts during the first 16 sec is due to field-aligned currents.

There is a noticeable variation in the data shown in Figure 4 with a periodicity of about 3.5 sec. The exact period is 3.456 sec and is due to the SSB/S instrument which is located 10 to 15 in. from the SSM sensors in the X direction. The SSB/S has an element that rotates about an axis parallel to the X direction. This element is suspended by a magnetic field so that it does not touch the rest of the instrument. This magnetic field varies slightly as the element rotates with a period of 3.456 sec. The variation is clearly seen in the SSM data. To determine the character of the signature from the SSB/S, the same SSM data shown in Figure 4 were detrended and folded back on themselves with a periodicity of 3.456 sec and are shown in Figure 5. As expected the 3.456 sec signature from the SSB/S is most noticeable in the X and Z component of the SSM data. However, there is another signature in Figure 5 with one-sixth the period of the SSB/S rotation. This comes from the six segments that make up the suspension magnetic field for the SSB/S rotating element. The 0.576-sec signature accounts for most, if not all, of the flipping in the least-significant bit (LSB) of the SSM data.

After the SSM raw data are received at AFGWC from various satellite tracking stations, the data are time tagged with Greenwich Mean Time (GMT) and ephemeris data at approximately one minute intervals are added to the SSM data records. Without any further processing, the SSM data are copied onto magnetic tapes and

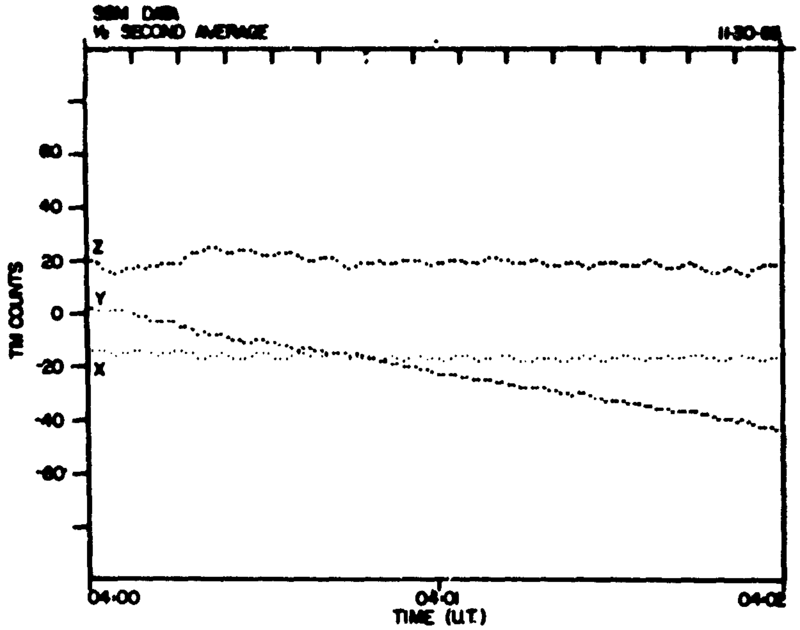

Figure 4. Two Minutes of Digital SSM Data From Part of the Same Period Shown in Figure 3. Each data point shown represents an average of 10 samples or 1/2 sec. The values have been shifted to display the three compoents on a common scale

mailed to AFGL. The digital data are received by AFGL in much the same format as received at AFGWC. Due to various factors, the data are not in a time sequence from earliest to latest. The data are edited at AFGL to put the data in proper time sequence and ephemeris data are interpolated to obtain these data at even 1-min intervals. Corrected geomagnetic coordinates, based on tracing the field line of the satellite down to 100 km altitude, are added to the ephemeris data. Finally, the data are copied onto new magnetic tapes for permanent archiving at AFGL and the original data tapes are sent back to AFGWC for recycling. At this point the SSM data are still in the form of counts in the compressed format shown in Table 2.

The magnetic field measurements in counts are transformed to values in nanoTesla by using the calibration values. The preliminary calibration values are 12.207 nT/count for all three axes. The final calibration was performed at the NASA Goddard Space Flight Center's 20-ft magnetic test chamber. The final calibration is only slightly different from the preliminary one. The calibration values are:

$$
\begin{array}{cccccccc}
\text{Measurement} & & \text{Calibration Coefficient Matrix} & & \text{Measurement} & & \text{Bias} \\
\text{(nT)} & & \text{(nT/count)} & & \text{(counts)} & & \text{(nT)} \\
\begin{bmatrix} Bx \\ By \\ Bz \end{bmatrix} & = & \begin{bmatrix} 12.1001 & -0.0055 & 0.0193 \\ -0.0247 & 12.1863 & -0.0101 \\ 0.0069 & 0.0232 & 12.1735 \end{bmatrix} & * & \begin{bmatrix} Bx \\ By \\ Bz \end{bmatrix} & - & \begin{bmatrix} 0.0653 \\ -59.8733 \\ -39.4228 \end{bmatrix}
\end{array}
$$

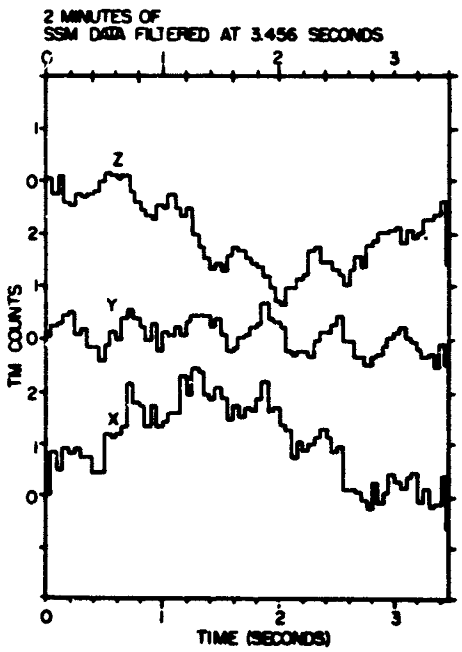

Figure 5. The 2 min of Digital Data Shown in Figure 4 Have Been Detrended and Folded Back on Themselves at a Period of 3.456 sec to Show the Effect of the Varying Magnetic Field Created by SSB/S

Various applications programs for processing the SSM data from the permanent archive tapes can be developed and run at AFGL. The most commonly run program generates a microfiche to show the deviations in the measurements from the expected ambient magnetic field. This procedure provides a "quick-look" format for surveying the data. This program is coded in two parts. The first part reads the archive tape and splits the bits so that each element of the SSM data for each second is in a separate integer word on the mainframe computer. These uncompressed data are written onto a temporary file and read back by the second part which makes the microfiche plot.

The second part of the standard processing program plots 25 min of data per plot or frame. The measured magnetic field components are reduced to 1-sec averages and converted from counts to nT. Because of all the uncertainties in the in-flight calibration and because the final calibration was not available until shortly before launch, the preliminary calibration is used for routine processing of the data. The difference between the measured and model field components is calculated for each 1-sec average measurement. The ambient magnetic field vectors are calculated from the International Reference Magnetic Field (IGRF80) model. Since there may be a semi-permanent spacecraft magnetic field and/or a constant offset to the output of the fluxgate sensors, the first valid data point for each axis in spacecraft coordinates is subtracted from all data for that axis during the 25-min interval plotted. The values of the first data points are shown at the right edge of the plot. The components are then plotted as shown in Figures 6 and 7.

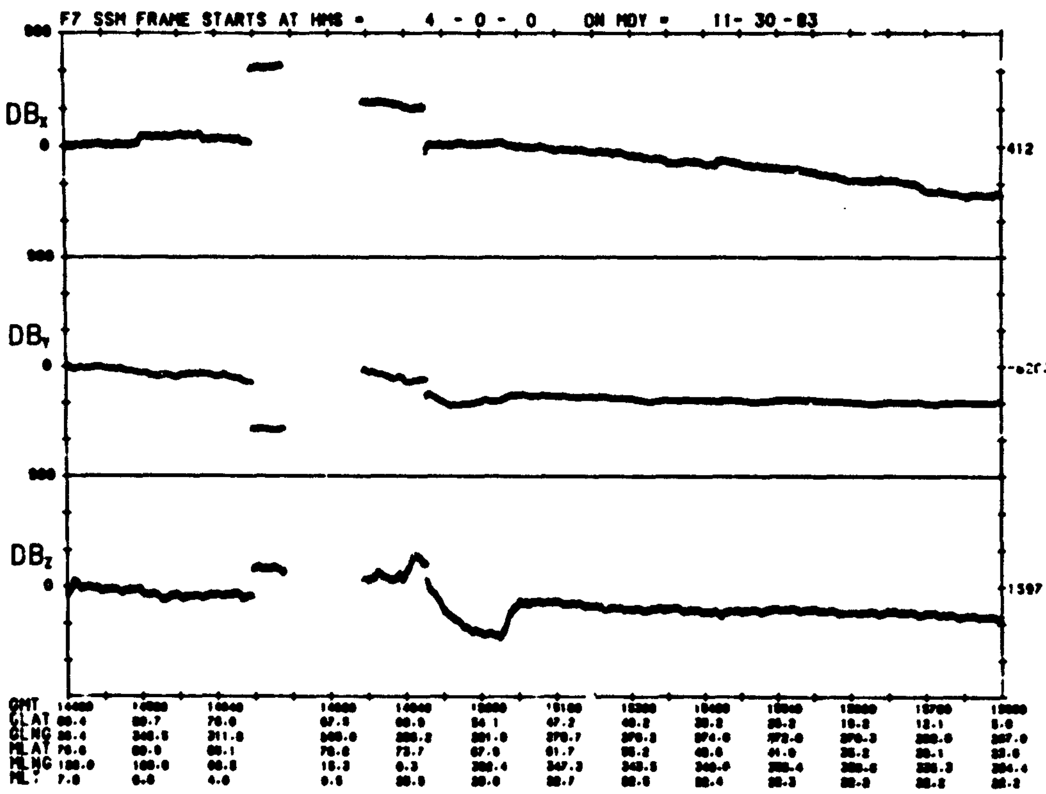

Figure 6a. Magnetic Deflection Data From the SSM in Spacecraft Coordinates Represent the Difference Between the Measured Magnetic Field and the Model or Expected Magnetic Field. This format is the standard plot for surveys of the data. These data are plotted in two frames of 25 min each. Frame a covers the time period 14400 sec (04:00) GMT to 15900 (04:25) GMT on 30 Nov 1983

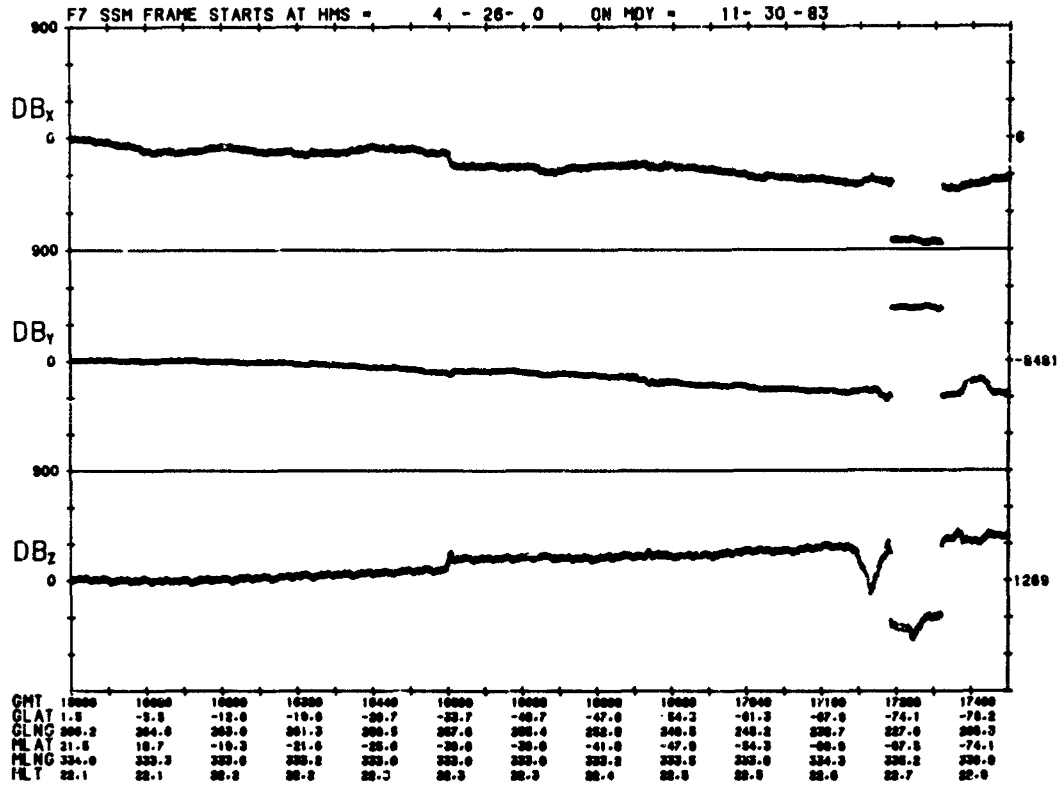

Figure 6b. Magnetic Deflection Data From the SSM in Spacecraft Coordinates Represent the Difference Between the Measured Magnetic Field and the Model or Expected Magnetic Field. This format is the standard plot for surveys of the data. These data are plotted in two frames of 25 min each. Frame b covers the time period 15960 sec (04:26) GMT to 17460 sec (04:51) GMT on 30 Nov 1983

In the plots that are routinely generated for surveys of the data, the components of the magnetic field deflections are given in spacecraft coordinates (Figure 1). If requested, the deflection vectors can be rotated about the model field vectors into geomagnetic coordinates. These coordinates are: X = outward and perpendicular to the model field (northward in the northern hemisphere); Y = eastward and perpendicular to the model field; and Z = parallel to the model field (downward in the northern hemisphere).

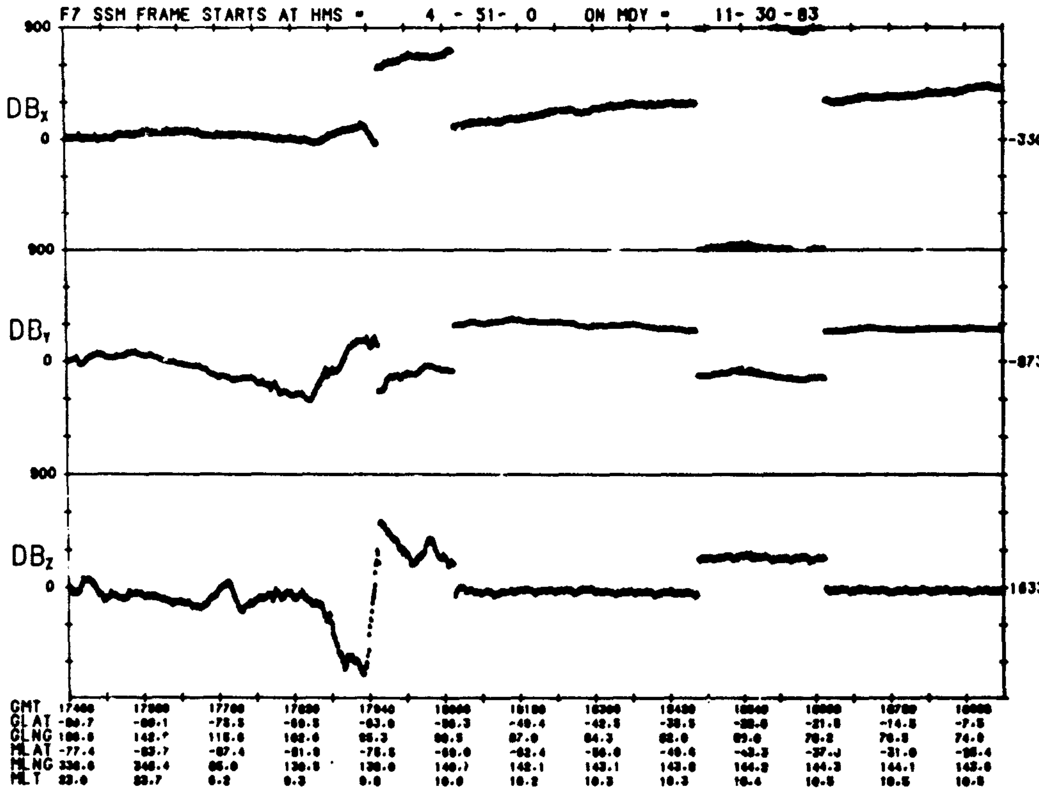

Figure 7a. A Continuation of the SSM Data From Figure 6. Frame a covers the time period 17460 sec (04:51) GMT to 18960 (05:16) GMT on 30 Nov 1983

The plots of the magnetic field data are divided into three sections, one for each component of the field deviation. Each section represents a range of +900 nT to -900 nT. If the value of one of the components of the deflection vector (after subtracting the first or base value) is outside the range of +900 nT to -900 nT, wrap-around logic is used to plot the data. In other words, 1800 nT is added to or subtracted from out-of-range values until they are within the range.

Each plot or frame represents 25 min of time. The size of the plot has been chosen to be the same as the standard plot for the SSJ/4 data. If there are missing data for 3 min or less, there will be a gap in the traces within a frame. These short gaps often occur when the spacecraft is transmitting to a ground station. If there are data gaps of greater than 3 min, the traces within the frame are halted at the start of the data gap and a new frame is started with the end of the data gap. This procedure is related to the need to interpolate the model field vectors from

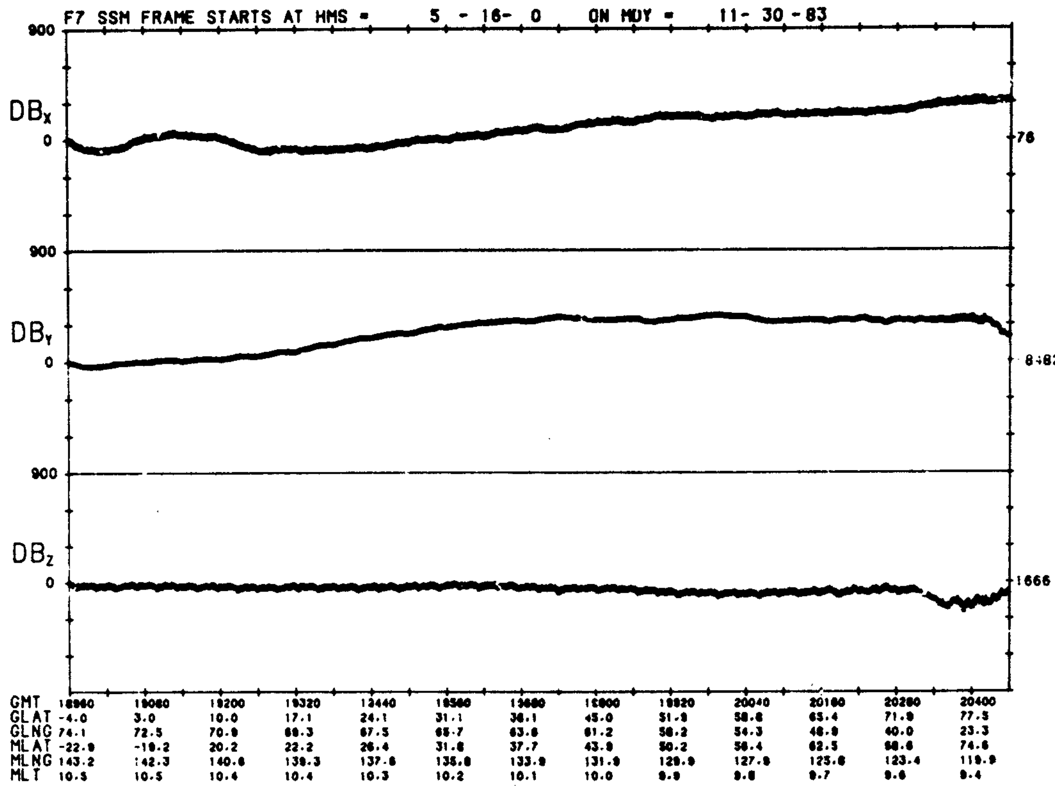

Figure 7b. A Continuation of the SSM Data From Figure 6. Frame b covers the time period 18960 sec (05:16) GMT to 20460 (05:41) GMT on 30 Nov 1983

the even minutes when ephemeris data is given to the time of a data point. Also, if there are 2 min or less of data with data gaps of greater than 3 min on both sides, the data will not be plotted.

The default option for standard processing yields plots of all available data. However, options exist within the standard procedure to plot only high latitude segments starting at the first minute poleward of 45 degrees magnetic latitude. Also, a plot can be made on microfiche or paper which starts at any time declared by the user.

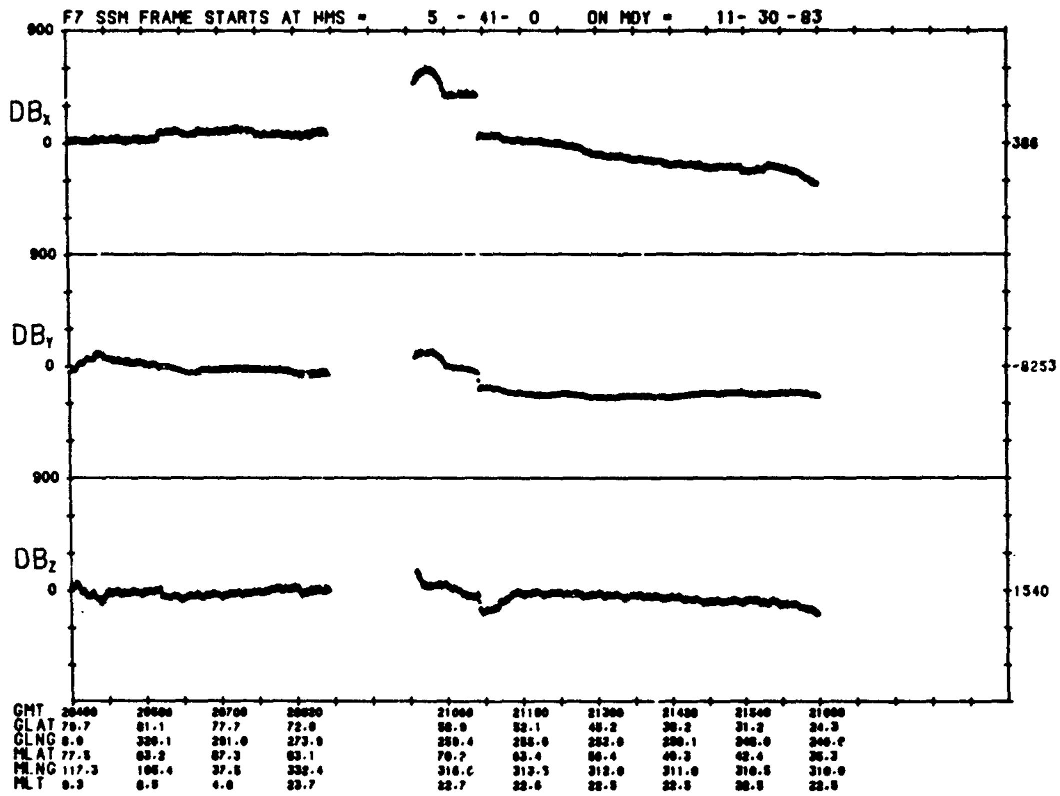

Figure 7c. A Continuation of the SSM Data From Figure 6. Frame c covers the time period 20460 sec (05:41) GMT to 21660 (06:01) GMT on 30 Nov 1983

6. EARLY ORBIT RESULTS

The first concern in analyzing the early orbit data was to determine whether or not spacecraft interference degrades the ability to detect geophysical disturbances with the SSM data. As we have shown above, only the SSB/S and the torquing coils have a noticeable effect. The signature from the SSB/S is very minor and can be completely removed if required. The signature of the torquing coil is a shift in the level of the measured magnetic field. As can be seen in Figures 6 and 7, geophysical disturbances can be clearly seen with the eye while the coils are on because the level shift is very constant with time. The level shift shown in the plots is less than the actual level shifts due to the wrap-around logic. Typical shifts are in the range of 3000 to 14,000 nT. In none of the early in-flight data has the shift been great enough to drive any axis of the sensor unit out of range.

After determining that the interference problem is negligible, we need to know if SSM is detecting geomagnetic disturbances. One of the major geomagnetic disturbances is the field-aligned current system associated with the auroral regions. Since the precipitating electrons and ions detected by SSJ/4 are major carriers of that current, the question is whether magnetic deflections observed by SSM correlate with precipitating particles. The answer is yes. For example, the magnetic deflections near 15060 sec GMT in Figure 6 and near 21120 sec GMT in Figure 7 correlate well with increased fluxes of precipitating particles as shown in Figures 8 and 9. For the South Pole pass shown in Figures 6 and 7, there are no SSJ/4 data available due to sunlight entering the SSJ/4 apertures.

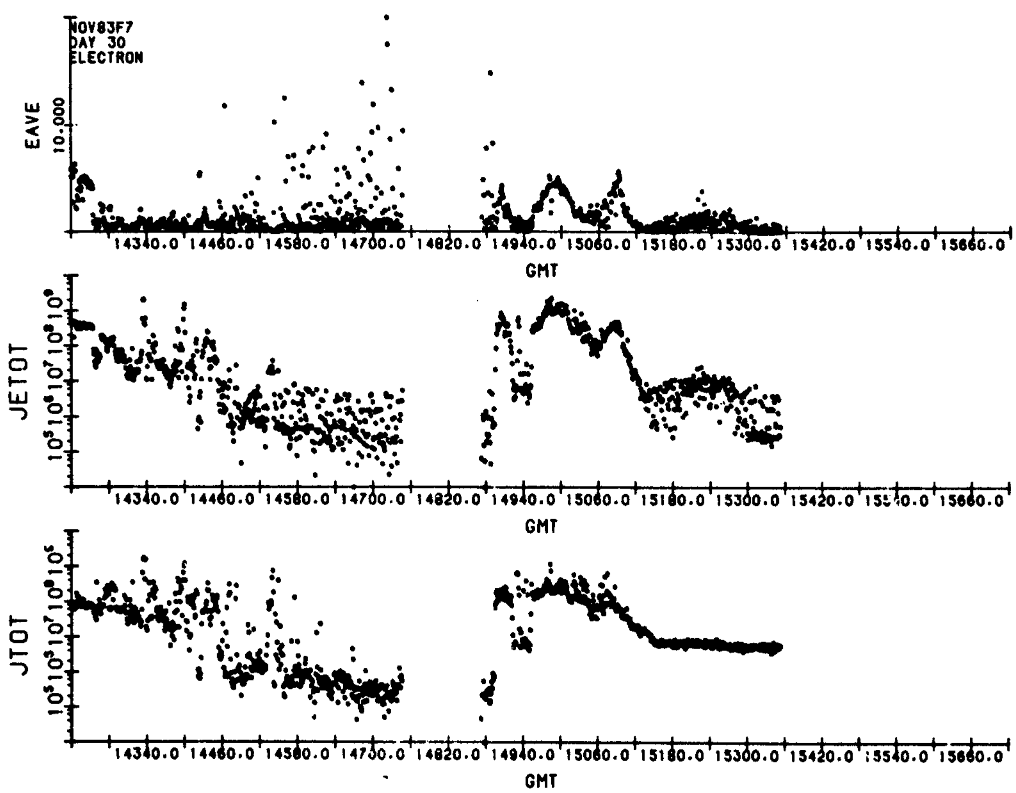

GLAT	78.5	81.2	79.0	73.8	67.5	60.9	54.1	47.2	40.2	0.0	0.0	0.0
GLON	43.1	4.8	324.4	303.1	293.0	286.2	281.9	278.7	276.2	0.0	0.0	0.0
MLAT	74.1	78.9	82.5	82.6	78.8	73.7	67.9	61.7	55.2	0.0	0.0	0.0
MLON	133.7	120.1	91.6	44.5	15.3	0.3	352.4	347.3	343.5	0.0	0.0	0.0
MLT	8.2	7.3	5.5	2.4	0.5	23.5	23.0	22.7	22.5	0.0	0.0	0.0

Figure 8a. Precipitating Particle Data From SSJ/4 for the Time Period 14220 sec (03:57) GMT to 15360 sec (04:16) GMT on 30 Nov 1983. The three traces in frame a represent precipitating 30 eV-to-30 keV electrons. The bottom trace JTOT represents the integrated number flux of particles in units of particles (cm^2 sec ster). The middle trace JETOT is the integrated energy flux in units of keV/(cm^2 sec ster). The top trace EAVE is the average energy in units of keV obtained by dividing JETOT by JTOT

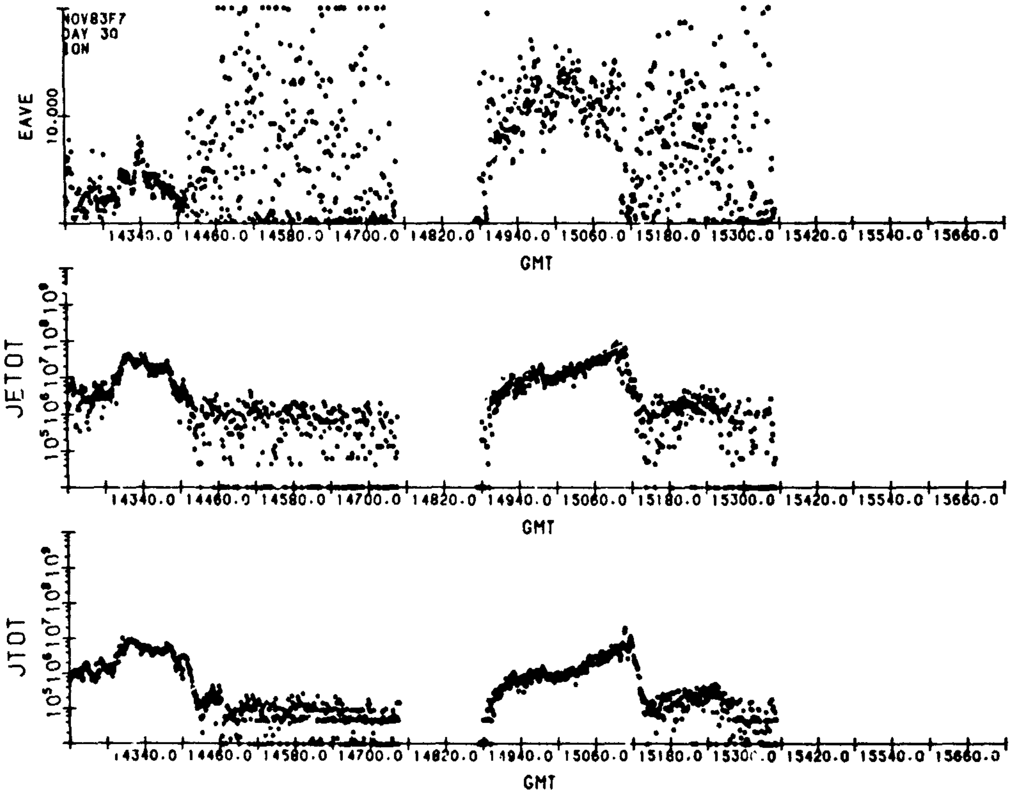

GLAT	78.5	81.2	79.0	73.8	67.5	60.9	54.1	47.2	40.2	0.0	0.0	0.0
GLON	43.1	4.8	324.4	303.1	293.0	286.2	281.9	270.7	276.2	0.0	0.0	0.0
MLAT	74.1	78.9	82.5	82.6	78.8	73.7	67.9	61.7	55.2	0.0	0.0	0.0
MLON	133.7	120.1	91.6	44.5	15.3	0.3	352.4	347.3	343.5	0.0	0.0	0.0
MLT	8.2	7.3	5.5	2.4	0.5	23.5	23.0	22.7	22.5	0.0	0.0	0.0

Figure 8b. Precipitating Particle Data From SSJ/4 for the Time Period 14220 sec (03:57) GMT to 15360 sec (04:16) GMT on 30 Nov 1983. The three traces in frame a represent precipitating 30 eV-to-30 keV electrons. The bottom trace JTOT represents the integrated number flux of particles in units of particles/(cm^2 sec ster). The middle trace JETOT is the integrated energy flux in units of keV/(cm^2 sec ster). The top trace EAVE is the average energy in units of keV obtained by dividing JETOT by JTOT

Are the correlations so perfect that the SSM data is redundant with the SSJ/4 data? The answer to that is, no. The particle fluxes, especially the electron flux, near 14900 sec GMT in Figure 8 is nearly as great as it is at 15060 sec GMT; yet the magnetic deflection shown in Figure 6 is rather small. This indicates that there are current carriers with energies outside the SSJ/4 energy range and/or outside the SSJ/4 field of view. Auroral phenomena are too complex for either SSM or SSJ/4 to fully describe the local activity.

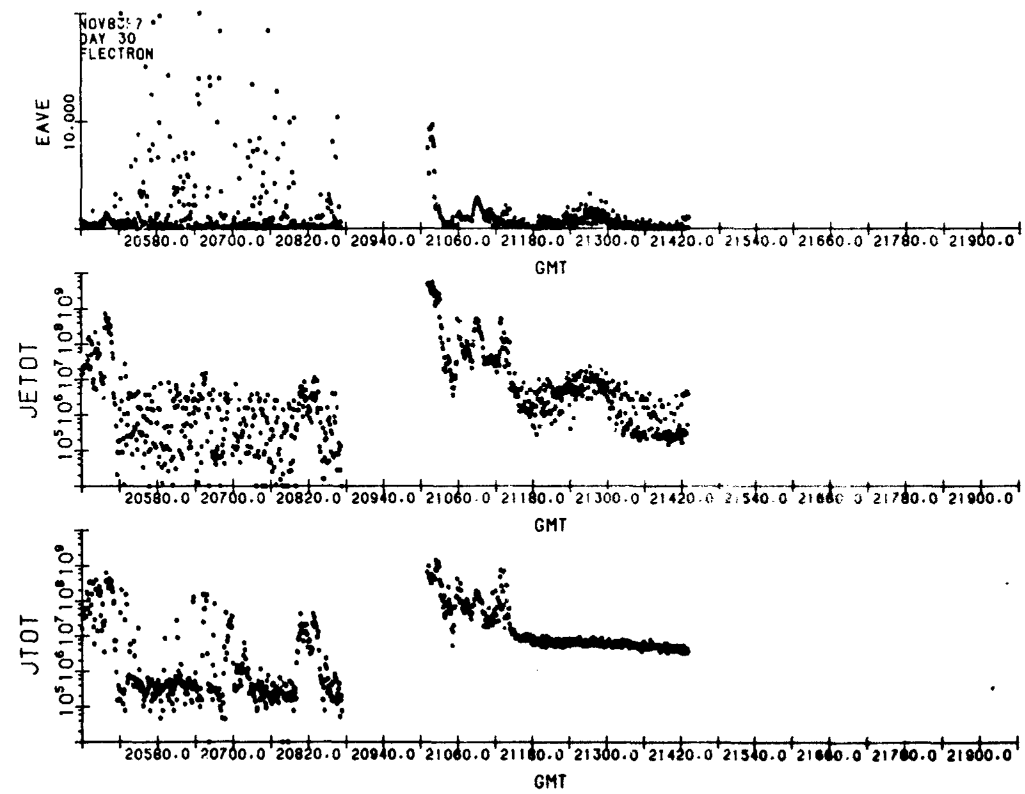

GLAT	81.1	77.7	72.0	62.3	58.9	52.1	45.2	38.2	0.0	0.0	0.0	0.0
GLON	326.1	291.0	273.9	262.0	259.4	255.6	252.6	250.1	0.0	0.0	0.0	0.0
MLAT	83.2	87.3	83.1	73.6	70.2	63.4	56.4	49.3	0.0	0.0	0.0	0.0
MLON	105.4	37.5	332.4	318.1	316.0	313.5	312.0	311.0	0.0	0.0	0.0	0.0
MLT	8.5	4.0	23.7	22.8	22.7	22.6	22.5	22.5	0.0	0.0	0.0	0.0

Figure 9a. Precipitating Electron Data From SSJ/4 for the Time Period 20460 sec (05:41) GMT to 21420 sec (05:57) GMT in the Same Format as Figure 8

Auroral activity is not uniform as a function of local time, especially during active periods. Thus, it is very valuable to be able to correlate the measurements of local activity with the visible light imagery. The imagery shows folds and spirals of the visible auroral bands that are related to dynamic events throughout the auroral zone. To give some clue to the correlations between the SSM data and the imagery, Figures 10 and 11 show examples of F6 imagery obtained at almost the same time as the SSM data shown in Figure 6 and SSJ/4 data in Figure 8. F7 imagery is not available for these early orbits. Figure 10 is an equatorward pass through the auroral zone at 0331 GMT. While the nadir portion of the imagery represents 18 hours magnetic local time, the whole image covers a wide range of

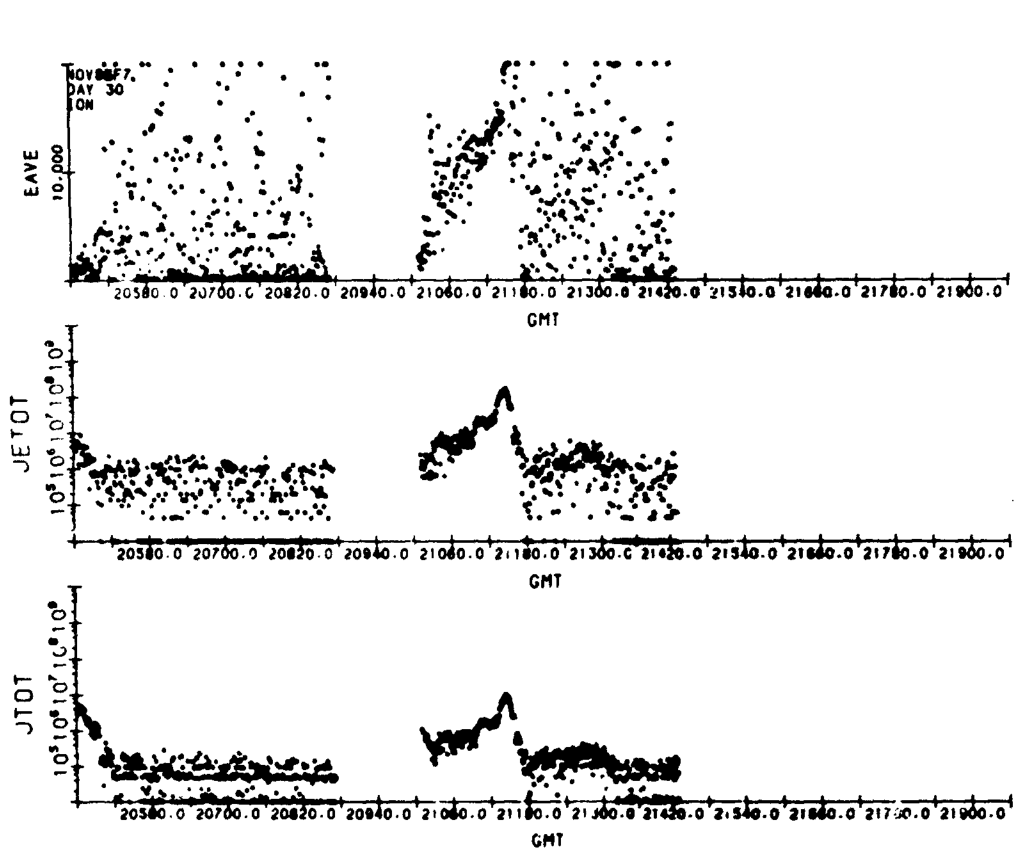

GLAT	81.1	77.7	72.0	62.3	58.9	52.1	45.2	38.2	0.0	0.0	0.0	0.0
GLON	326.1	291.0	273.9	262.0	259.4	255.6	252.0	250.1	0.0	0.0	0.	0.0
MLAT	83.2	87.3	83.1	73.6	70.2	63.4	56.4	49.3	0.0	0.0	0.	0.0
MLON	105.4	37.5	332.4	318.1	316.0	313.5	312.0	311.6	0.0	0.0	0.	0.0
MLT	8.5	4.0	23.7	22.8	22.7	22.6	22.5	22.5	0.0	0.0	0.0	0.0

Figure 9b. Precipitating Ion Data for SSJ/4 for the Time Period 20460 sec (05:41) GMT to 21420 sec (05:57) GMT in the Same Format as Figure 8

local times. In particular, the region near 23 hours magnetic local time, which the F7/SSM data in Figure 6 represent, is clearly visible in Figure 10. Likewise, Figure 11 is a poleward pass through the auroral zone at 0500 GMT with nadir at 06 hours magnetic local time, and it shows some of the auroral region near 08 hours magnetic local time represented in the SSM data in Figure 7. In this particular case, the relationship between the images and the SSM data seems relatively simple because activity was moderate to low.

Several studies have already related the SSJ/3 data to the white light images and other indicators of auroral activity, and the understanding of the aurora has been increased. With SSM in addition to SSJ/4 and the images, new studies can be undertaken which will increase our understanding of the complex events related to the auroral zone.

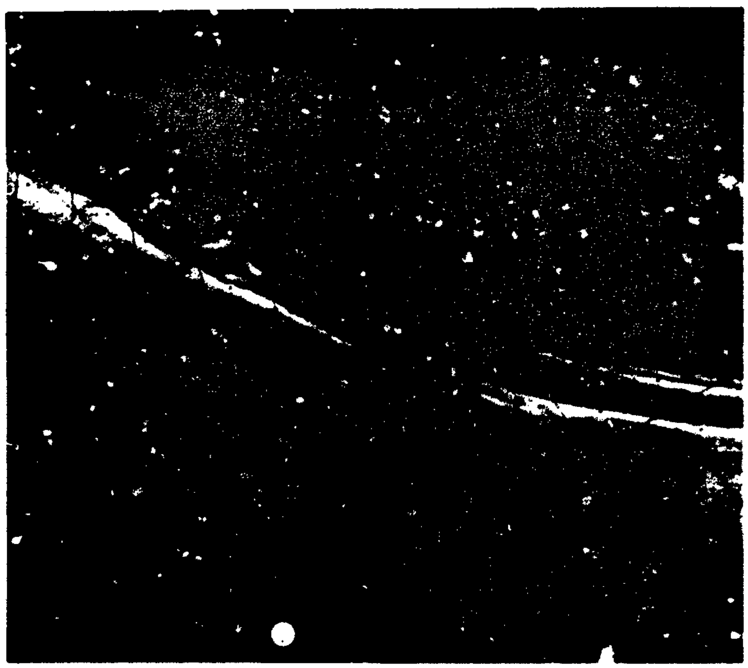

Figure 10. White Light Imagery From the F6 Operational Line Scanner (OLS). F6 crossed the evening auroral zone southbound at 0331 GMT and 1800 magnetic local time (MLT) over northwestern Canada. Forty minutes later, F7 passed through the auroral zone at 2300 MLT. The F7 data are presented in Figures 6 and 8

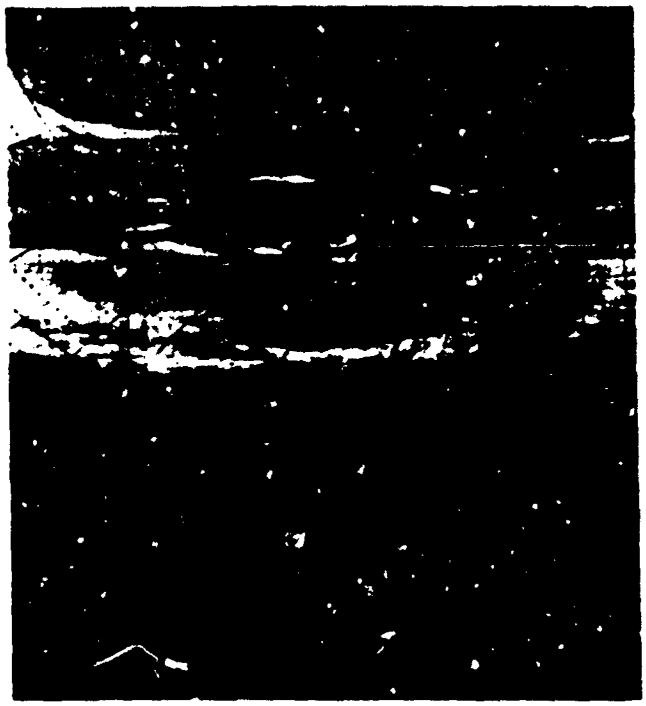

Figure 11. White Light Imagery From the F6 Operational Line Scanner as it Crossed the Morning Auroral Zone Northbound at 0500 GMT and 0600 MLT over the North Atlantic off Norway. Forty minutes later, F7 passed through the auroral zone at 0900 MLT. The F7 data are presented in Figure 7